Investigating root architectural differences in lines of Arabidopsis with altered stomatal density using high resolution X-Ray Synchrotron imaging.

Tinashe Mawodza (tinashe.mawodza@nottingham.ac.uk)
University of Sheffield https://orcid.org/0000-0002-2729-5107
Manoj Menon
Nancy Muringai
Oxana V Magdysyuk
Genoveva Burca
Stuart Casson

Research Article

Keywords: Arabidopsis thaliana, X-Ray synchrotron Imaging, Root architecture, Water use efficiency, Neutron imaging

Posted Date: May 4th, 2022

DOI: https://doi.org/10.21203/rs.3.rs-1566117/v1

Abstract

Purpose

Freshwater is an increasingly scarce natural resource, essential for agricultural production. As plants consume 70% of the world's freshwater, a reduction in their water use would greatly reduce global water scarcity. Plants with improved Water Use Efficiency (WUE) such as those with altered expression of the Epidermal Patterning Factor (EPF) family of genes regulating stomatal density, could help reduce plant water footprint. Little however, is known about how this modification in Arabidopsis thaliana affects root architectural development in soil, thus we aim to improve our understanding of this growth.

Methods

We used X-Ray synchrotron and neutron imaging to measure in three dimensions, the root system architecture (RSA) of Arabidopsis plants of three different genotypes, namely that of the wild type Columbia (Col 0) and two different EPF mutants, EPF2OE and *epf2-1* (which show reduced and increased stomatal density respectively). We also used total biomass and carbon isotope discrimination (Δ) method to determine now WUE varies in these genotypes when grown in a sandy loam soil under controlled conditions.

Results

Our results confirm that the EPF2OE line had superior WUE as compared to the wild type using both the Δ and total biomass method. The *epf2-1* mutant on the other hand, had significantly reduced WUE using the Δ but not in the biomass method. In terms of root growth, the RSA of the different genotypes had no significant difference between each other. There was also no significant difference in rhizosphere porosity around their roots as compared to bulk soil for all genotypes.

Conclusions

Our results indicate that the EPF mutation altering stomatal density in Arabidopsis plants did not have an adverse effect on root characteristics thus their wide adoption to reduce the global freshwater footprint is unlikely to compromise their soil foraging ability.

1. Introduction

Persistent water shortages and scarcity are major global challenges that affect the livelihoods of more than half of the world's population, many of whom live in the least developed parts of the world (FAO 2020, UNESCO 2021). The prudent use of the increasingly limited freshwater resources available especially in water scarce regions is necessary to maintain food security and general quality of life. As

agriculture is predominantly the largest withdrawer of global freshwater resources, accounting for close to 70% of all freshwater withdrawals, strategies that maximise agricultural water utility are paramount to reducing global water scarcity (Hoogeveen et al. 2015, Gleick and Cooley 2021). Reducing the water used for the irrigation of crop plants is one such promising strategy that could help optimise agricultural water use. This is because irrigation accounts for the bulk of the water used by modern agriculture and as such, even a marginal decrease in plant water use could result in a noticeable decline in agricultural freshwater consumption (de Avila et al. 2015, Cao et al. 2021).

Numerous strategies to improve the efficiency of freshwater use by plants have been developed with some showing great promise for enabling a more sustainable path for agricultural water use management. Of these interventions, one of the most interesting is through the genetic manipulation of stomatal density, which has been shown to improve both drought resistance and Water Use Efficiency (WUE) in plants through limiting transpiration, which is the main source of water loss from plants (Bertolino et al. 2019, Buckley et al. 2020). Reducing stomatal density by manipulating the expression of different members of the Epidermal Patterning Factor (EPF) family of genes has been demonstrated to confer improved drought resistance and water use efficiency. This has been shown to be the case in Arabidopsis (Franks et al. 2015, Hepworth et al. 2015, 2016), barley (Hughes et al. 2017), rice (Caine et al. 2019, Mohammed et al. 2019) and wheat (Dunn et al. 2019). The wide use of this strategy could potentially decrease the water footprint associated with plant productivity and thus have a great impact in dealing with the prevalent global water shortages.

Despite the beneficial traits of manipulating the EPF genes, little is known about how changes in stomatal density affect root architectural development with only a few papers like Mohammed et al. (2019) showing how changes in the EPF1 gene affect rice root aerenchyma. This deficit in studies looking at root properties is mainly due to the fact that roots are often obscured within opaque soil and thus are frequently neglected as they are not easily studied using traditional methods of plant analysis. This is even more apparent in the model plant, Arabidopsis, which is a relatively small plant whose root properties when grown in soil are seldom measured in literature. In many of the Arabidopsis experiments, roots are often grown in colourless growth media such as agar gel (French et al. 2009, Xiao et al. 2015), hydroponic solutions (Dayod et al. 2013, Strehmel et al. 2014) or even artificially synthesised transparent “soil” (Downie et al. 2012, Ma et al. 2019). Although these techniques provide useful insights into how specific gene alterations may affect root growth, they lack a specific dimension patterning to the actual performance of Arabidopsis roots in soil, their natural growth media, soil.

Studying Arabidopsis root properties in soil using the traditional method of root washing is difficult due to the fact that Arabidopsis roots are very thin (48–150μm thickness) and fragile, resulting in significant losses during the washing process. As an alternative, some researchers have resorted to using angled plastic rhizotrons with uniformly graded sand, encouraging the roots to grow at the glass sand interface for ease of visualisation (Chapman et al. 2011). Hepworth et al. (2016) used vermiculite containing rhizotrons covered with a glass microfiber paper that prevented direct contact between Arabidopsis roots and the growth media thus enabling easy separation and analysis of the roots. All these techniques

however do not give a true representation of how Arabidopsis plants would grow in natural environments. To counter for the challenges faced by the traditional root-soil analysis methods, Lucas et al. (2011), Seignez et al. (2010), Tracy et al. (2010) and more recently Morris et al. (2017) used more advanced X-Ray CT scanning to reveal Arabidopsis roots in natural soil. Most of these studies, however, did not reveal the entirety of the root architecture of the Arabidopsis plant. In the case of Lucas et al. (2011) (scan resolution18 μm $pixel^{-1}$), the researchers resorted to using other non-soil based methods to quantify root architectural properties in the mutants they studied whilst Tracy et al. (2010) (scan resolution16μm $pixel^{-1}$) only as a proof of concept showed only a single grayscale image of an arabidopsis without attempting to segment out the roots in the image. Seignez et al. (2010) (scan resolution 10μm $pixel^{-1}$) on the other hand in a soil pollution study investigated only a small root section of *Arabidopsis halleri* (Similar genus to *Arabidopsis Thaliana*) in contact with contaminated soil as opposed to revealing the entire root architecture of the plants grown. Only Morris et al. (2017) (scan resolution not specified) in a review looking at how roots are shaped by different stimuli by goes into greater detail of arabidopsis root architecture. In this study they looked at a time series of growth of an Arabidopsis seedling growing in soil for a 21 day period. Even in this experiment however, less than half of the entire core was scanned to reveal root architecture, leaving out a significant portion of the growing roots unimaged.

In-spite of the challenges associated with studying Arabidopsis in mineral soil as outlined above, here we aim to use soil based systems to better understand the consequences of alterations in stomatal density via manipulation of the EPF family of genes on root properties in Arabidopsis. This study compares three different Arabidopsis lines with differing stomatal densities; the wild-type control (Col-0), *epf2-1* (a mutant that has an increased stomatal density) and EPF2OE (a transgenic line that overexpresses *EPF2* gene resulting in greatly reduced stomatal density). Our specific objectives were to (a) Estimate the WUE of the EPF mutants as compared to wild type plants when grown under controlled conditions in soil using biomass and Δ methods, (b) Reveal whole root architectural properties of the different Arabidopsis lines when grown in soil using high-resolution synchrotron imaging scanning as well as Neutron CT and (d) Compare how the roots of these different lines interact with the soil pores.

2. Methods And Materials

2.1 Plant growth conditions

Three *Arabidopsis thaliana* (L.) Heynh genotypes were used in this study. These were the wild type Col-0 (used as control) and two stomatal mutants *epf2-1* and EPF2OE all derived from the Col-0 background as described in Hunt & Gray, (2009). Prior to plant growth, seeds were stratified at 4°C for 48hours before being transferred to a controlled growth chamber maintained at a temperature of 22°C (day)/18°C (night) (SD ± 2°C) and at a relative humidity of 55% with a 9 hour day length. A sandy loam soil (70% Sand, 16% Clay and 14% Silt) obtained from Cove farm (53°30'03.7"N 0°53'57.2"W) with an organic carbon content of 4.18 ± 0.18 was used in this study. This was sieved over a 2mm sieve to eliminate coarse particles and packed in the necessary pots/containers to a bulk density of 1.2 $g.cm^{-3}$.

The plants were grown at a distance of 30cm (maximum) from the light source receiving light averaging 180 µmol m^{-2} s^{-1} (± 15 µmol m^{-2} s^{-1}) in intensity at plant height. Watering was done every 3–4 days to ensure that the water content was maintained a volumetric water content between 20 and 25% for the duration of the growth experiments. The Arabidopsis plants used were grown for between 6–8 weeks depending on the analysis to be done after their growth.

2.2 Stomatal density

Stomatal impressions using resin (Coltene, PRESIDENT) were done on the abaxial surface of 3 fully expanded leaves per plant with at least 4 plants of each genotype used. These impressions were embedded on a microscope slide using clear tape and Z-stack images were taken under a Leica DM IRBE Inverted Microscope (20x/ 0.4∞/ 0.17-A). Z-stack files obtained from microscopy were opened using ImageJ software (v.1.52p) and numeration of abaxial stomata was done using the count tool. As stomatal properties vary along the leaf surface, to attain a more uniform characterisation of stomatal properties, the leaves were divided into 3 equal sections as illustrated in Fig. 1. The total number of stomata for each of the different sections were counted and the average number of stomata across the entire leaf was determined. The average stomatal counts were then used to calculate stomatal density (SD) per mm^2 of leaf area using the formula:

$$SD = \frac{TotalEquationNumberofstomata}{mm^2}$$

1

2.3 Water use efficiency estimation

WUE in this study was estimated using two different methods, namely using the ratio between total dry biomass and water lost via evapotranspiration as well as the carbon isotope discrimination (Δ) method. In the biomass ratio method, the total dry biomass was measured after drying all the plant tissues at 60˚C for 48 hours and the total amount of water lost via evapotranspiration during the growth of a plant. To reduce soil surface evaporation, a transparent plastic sheet was placed on the surface of the soil surrounding each plant. The carbon isotope discrimination method, on the other hand involved using plant leaves to determine the WUE of a particular plant, these were sampled from at least 3 mature leaves from each plant at the same developmental stage for each different plant species. The sampled material was oven-dried at 65°C for 48 hours then ground using a ball bearing in a tissue lyser machine to a fine powder. This powder was then used to determine the $^{13}C/^{12}C$ carbon ratio using an ANCA GSL 20–20 Mass Spectrometer made by Sercon PDZ Europa (Cheshire, United Kingdom). The sample $\delta^{13}C$ results reported by the machine were not absolute measurements but indicated the difference between our given samples (R_{sample}) vis a vis the standard Vienna Pee Dee Belemnite (PDB) ($R_{standard}$). The sample δ13C was then calculated using the formula specified in Farquhar et al. (1989) that is as follows:

$$\delta^{13}C_{sample} = \left(\frac{R_{sample}}{R_{standard}} - 1 \right) \times 1000$$

3

The C isotope discrimination (Δ) of each plant sample was then calculated using the formula:

$$\Delta^{13}C = \frac{\delta^{13}C_{air} - \delta^{13}C_{sample}}{1 + \delta^{13}C_{sample}}$$

4

Where $\delta^{13}C_{air}$ was obtained from at least five samples of air taken from the growth chamber where the plant material analysed was grown.

2.4 Synchrotron X-Ray computed tomography (sX-ray CT)

The Arabidopsis plants used in the sX-ray CT experiments were grown for 26 days after sowing in cylindrical polyvinyl chloride (PVC) tubes (36 mm diameter, 70 mm height). sX-ray CT was done using the I12-JEEP beamline (Drakopoulos et al., 2015) at the Diamond Light Source facility (UK) using a monochromatic beam with an image resolution of 7.91 µm per pixel (FOV = 20 mm×12 mm). A double field of view scan was employed with a total of 8 scans being done to cover the entire core used for plant growth as illustrated in Fig. 2. A total of 11 cores were scanned with at least 3 scans being done for each genotype. Tomographic reconstruction was performed using the SAVU system (Atwood et al. 2015, Wadeson and Basham 2016). A filtered back projection (FBP) algorithm was also used (Ramachandran and Lakshminarayanan 1971), as implemented in the ASTRA toolbox (van Aarle et al. 2016).

2.5 Neutron tomography

As an alternative method for imaging Arabidopsis root architecture that would make root segmentation easier, we used neutron tomography. This imaging method is often considered complementary to X-Ray tomography as it can accentuate subtle low density components such as water (contained in roots), that are not easy to identify in X-Ray CT scans. The tubes used for X-ray CT were unsuitable for measurements with neutron imaging as they were made of PVC plastic which is highly neutron attenuating. As a result we used aluminium cylinders (10mm diameter, 14mm height) for neutron computed tomography (NCT) measurements. The Arabidopsis plants grown were grown for 28 days. Neutron imaging was carried out at the IMAT neutron imaging and diffraction beamline of the ISIS neutron spallation source at the Rutherford Appleton Laboratory (UK) (Burca et al. 2018) using an optical camera box equipped with a 2048 × 2048 pixels (each pixel of 55µm) Andor Zyla 4.2 PLUS sCMOS camera for a standard white beam neutron tomography with 0.7-7 Å wavelength range. Scanning was performed following a modified version of the protocol similar to that described in Mawodza et al. (2020).

The scanning of the cylindrical containers was done with a rotation step of 0.913° for each projection with an exposure time of 30 sec per radiography resulting in 394 projections over 3 hours of measurement. Two samples were scanned simultaneously with a multiaxial tomography stage equipment available at ISIS (Burca, G., Private communication 2020).

2.6 Image processing and analysis

The reconstructed scans from both sX-ray CT and NCT were saved as two dimensional cross sectional images of the scanned plants which were imported into either Image J (Schneider et al. 2012) or Avizo 9.0.1 (FEI 2015) for further processing. The 8 individual stacks for each plant from sX-ray CT were aligned and merged into a single stack. As noise was minimal and image sizes were large (> 20 Gb) in the sX-Ray, a 3×3 median filter which required minimal processing was used prior to root segmentation. On the other hand, for NCT images, a non-local means filter was used to eliminate noise prior to segmentation. Automated root segmentation techniques using algorithms such as Root1 in ImageJ as well as Rootrak were attempted but these were unable to successfully segment out the roots from sX-ray CT. As a result we used a combination of manual tracing which involves physically selecting root pixels from each of the slices that make up the 3D image as well as the interpolating algorithm in Avizo to extract the entire root architecture. As roots were clearer in NCT, the majority of the segmentation was carried out using the Root1 algorithm in ImageJ. The results of this segmentation were imported into Avizo and additional manual segmentation was carried out to enhance the automated segmentation. Due to the considerable moisture within the tubes used for NCT however, extracting the entire root system was not possible. For sX-ray CT root length, lateral root number, root thickness, convex hull and root volume were determined using the modules in Avizo whilst root angle was determined in an exported BMP file using the Rooth software. Convex hull in this study was defined as the smallest convex set of pixels that contains all other pixels in the root system (Iyer-Pascuzzi et al. 2010). This volume can be used to define the potential for soil exploration of the soil by a root system (Helliwell et al. 2019)

To differentiate between soil under the influence of the root and the rest of the soil, a cylindrical soil mask within a radius of 390μm from the centre of each root was defined as being in the rhizosphere whilst the rest of the soil was defined as bulk soil as shown in (Fig. 3). This is in line with measurements made by Ortas (2008) in sorghum. This measurement was done on the entire rooting system of each of the plants.

2.7 Statistical analysis

The analysis of the results from these experiments was carried out using Graphpad prism v9.0 (GraphPad Software, LLC). Assumptions of normality and homogeneity of variance were performed using Shapiro-Wilk and Bartlett tests respectively. A one way ANOVA was used to explore the difference in means with a post hoc Bonferonni test used to separate between means.

3. Results

3.1 Stomatal characteristics

Abaxial stomatal properties showed considerable differences between the genotypes as expected. Stomatal density (SD) (Fig. 4D) in the *epf2-1* mutant was around 300 stomata/mm^2 which was approximately 44% higher as compared to the wild type which had a stomatal density of 200 stomata/mm^2. On the other hand the EPF2OE mutant had a SD of 55 stomata/mm^2 which represented a reduction of 73% reduction in stomata as compared to the wild type.

3.2 Water use efficiency

In terms of water use efficiency, significant differences in Δ (Fig. 4A) were found between both the mutants as compared to the wild type plants with the epf2 mutant showing significantly increased Δ, indicating lower WUE whilst the EPF2OE lines showed significantly reduced Δ indicating improved WUE. Complimentary to this, WUE measurements in terms of biomass production per unit water loss (Fig. 4B) also showed a significant increase in WUE for the EPF2OE line plants over a 50 day growth period in comparison to the wild type plants. Unexpectedly, however, there was no significant decrease in WUE of the epf2 mutant as estimated using this method despite the significant increase in Δ. The WUE of this mutant was only marginally lower than that of the wild type plants.

3.3 Root architectural properties

Determining root architecture from neutron imaging proved difficult as the contrast between Arabidopsis roots and soil was not pronounced. Only parts of the primary root (Fig. 6) could be visualised in our experiment, which limited our inferences from NCT. On the other hand, images from sX-Ray CT, which had higher resolution, were able to reveal both primary and lateral roots in detail (Fig. 6). Our segmentation of sX-Ray CT images resulted in a detailed three dimensional root networks from which root properties could be determined with up to 2nd order lateral roots being segmented from our scans. There were no significant differences in root length, volume, diameter and angle between the different mutants as compared to the wild type (Fig. 8A-D). The most striking difference, however, was between lateral root densities of the EPF2OE mutants as compared to the wild type and *epf2-1* mutants. This was about 30–35% lower than that of the other genotypes.

3.4. Roots interactions with the soil pores

The porosity of the bulk soil was generally lower as compared to soil in the rhizosphere. There was however no significant difference between the porosity of the rhizosphere soil between the different genotypes with an average porosity of around 40.8% in the rhizosphere and 38.6% in the bulk soil for all genotypes (Fig. 9). There was also no significant difference in porosity between the bulk soil used to grow all the different genotypes in this experiment.

4. Discussion

In this study, we examined the impact of altering stomatal density (and consequently WUE) on the root architecture of Arabidopsis plants. We were able to visualize Arabidopsis RSA in much greater detail as compared to most other studies done previously as we took advantage of high energy synchrotron X-

Rays to obtain high resolution (7.9μm pixel^{-1}) scans of roots growing in a mineral soil. We were also able to make inferences on how the roots of EPF mutants interacted with soil structure as we obtained three dimensional maps of root-soil interactions for all the plants used in our study.

As expected, stomatal density in the EPF2OE lines with increased expression of the *EPF2* gene had severely reduced SD as compared to the wild type. This is similar to what was observed by Hepworth et al. (2015) and Lundgren et al. (2019) who reported a SD reduction of between 60 and 65% in the same genotype as compared to a 73% difference in this case. On the other hand, the SD of the *epf2-1* mutant was 44% higher than that of the wild type which was relatively lower than that reported by Hunt and Gray (2009) who reported a 70% increase in the same genotype. The differences in SD in this study as compared to previous studies may have been due to the use of different growth media (mineral soil) used in this study instead of compost. This change may have had an effect of altering root-soil interactions which could have affected leaf cell developmental expression thus altering SD to some extent.

In line with our SD results, the EPF2OE line showed significantly improved WUE as compared to the wild type using both the carbon isotope discrimination (Δ) and biomass method of measuring WUE. This was probably as a result of reduced transpiration from the leaf surface which conserved water within the leaves. Also as anticipated, using the Δ method, the WUE of the *epf2-1* mutant with increased stomatal density had significantly reduced WUE as a result of the increased SD. Surprisingly however, there was no significant difference in WUE between the wild type plants and the *epf2-1* as calculated from biomass and total water transpired. This could possibly be explained by the improved water conservation that could have occurred as the soil dried quicker when *epf2-1* plants were grown which may induce a drought response would have the consequence of limiting transpiration to some degree.

Imaging of Arabidopsis roots using NCT proved quite challenging as the size of the roots (≈ 80 μm) was too small to enable near complete root segmentation from the resolution we achieved (55μm pixel). Also a delicate balance between amount of water applied and what would be optimal for NCT was difficult to achieve as Arabidopsis roots dry quite rapidly as compared to other plants limiting how dry the soil can be during imaging. Only the main taproot near the surface of the soil was visualised and thus we focused RSA assessments more on results of sX-Ray CT. The sX-Ray CT scans revealed much greater detail of the Arabidopsis roots as compared to previous studies using soil as a growth media e.g. Morris et al. (2017). The root properties indicated that there was generally no difference between the different root architectures of the three different genotypes grown. This is contrary to what was found by Hepworth et al. (2016) who observed a generally reduced RSA in EPFOE mutants as compared to wild type plants. There was also no significant RSA difference between wild type and the *epf2-1* mutant with higher SD which was also contradictory to findings by Hepworth et al. (2016) albeit using a different genotype i.e. (*epf1epf2*) a double mutant with much higher SD in comparison. Although the differences that were shown were insignificant, the EPF2OE mutant however tended to have the smallest RSA and reduced lateral root density which partially supports Hepworth et al. (2015)'s findings who postulated that the reduced transpiration tended to reduce root growth. The potential differences that could have been observed in this experiment may however, have been made moot by the non-uniform nutrient distribution

within the soil used which may have influenced root growth. It is noteworthy that in mineral soils such as in this experiment, roots exhibit a greater degree of plasticity thus variation in root architecture may be more difficult to definitively asses with relatively few replicates as in our case. The plants used in this study were also younger (26 days) as compared to those assessed in Hepworth et al. (2016) (35days) thus further complicating comparison between our experiments.

The interaction between Arabidopsis roots and the soil for all the mutants was generally similar with roots tending to be located in areas with slightly higher porosity as compared to the rest of the soil. For this characterisation however, an arbitrary estimation of rhizosphere was made with a diameter of about 390µm around the roots based on the lower end of the zone suggested by Ortas (2008) who worked on sorghum roots. This could have a slight impact on our findings as Arabidopsis has a relatively smaller root system and thus potentially a smaller rhizosphere. Our classification, however, provided a guide into what the soil pore characteristic that were under the effect of the roots.

In general, our results did not show any adverse effects associated with the WUE coffering EPF2 overexpression as in the EPF2OE mutant. This suggested that alteration in the EPF family of genes could be a suitable way of improving WUE without affecting rooting characteristics and thus enabling sustainable production of plants with altered stomatal development, though this would need to be experimentally determined for different crop species with larger root systems.

5. Conclusions

This study reaffirmed the idea that improvement in WUE as brought about by a reduction in stomatal density in well-watered conditions as shown in previous studies. We also showed that investigations on Arabidopsis roots growing in soil can be successfully carried out using high resolution XRSI as there weren't any major differences in root architectural properties between the genotypes. These results potentially indicate that cultivation of water use efficiency with alterations in the *EPF2* gene and hence stomatal density, does not impact soil properties. There is therefore the potential to generate more sustainable crops with improved WUE without any negative impacts on soil properties.

Abbreviations

WUE=Water Use Efficiency, EPF= Epidermal Patterning Factor, SXCT = X-Ray Synchrotron Computed Tomography, NCT= Neutrons Computed Tomography, Carbon isotope discrimination = Δ, RSA = Root system Architecture

Declarations

Acknowledgements

This research was funded as part of a PhD studentship by the Grantham Centre for Sustainable Futures at the University of Sheffield. Neutron imaging beamline grant (RB1910228) was provided by STFC ISIS Facility (doi:10.5286/ISIS.E.RB1820361) as well as the I12 beamline (proposal mg22992) at Diamond Light Source Ltd., UK.

References

1. van Aarle W, Palenstijn WJ, Cant J, Janssens E, Bleichrodt F, Dabravolski A, De Beenhouwer J, Batenburg J, Sijbers J (2016) Fast and flexible X-ray tomography using the ASTRA toolbox. Opt Express 24(22):25129
2. Atwood RC, Bodey AJ, Price SWT, Basham M, Drakopoulos M (2015) A high-throughput system for high-quality tomographic reconstruction of large datasets at Diamond light source. *Philosophical Transactions of the Royal Society A: Mathematical, Physical and Engineering Sciences*, 373 (2043)
3. de Avila LA, Martini LFD, Mezzomo RF, Refatti JP, Campos R, Cezimbra DM, Machado SLO, Massey JH, Carlesso R, Marchesan E (2015) Rice water use efficiency and yield under continuous and intermittent irrigation. Agron J 107(2):442–448
4. Bertolino LT, Caine RS, Gray JE (2019) Impact of Stomatal Density and Morphology on Water-Use Efficiency in a Changing World. Front Plant Sci 10(March):225
5. Buckley CR, Caine RS, Gray JE (2020) Pores for Thought: Can Genetic Manipulation of Stomatal Density Protect Future Rice Yields? Front Plant Sci 10:1783
6. Burca G, Nagella S, Clark T, Tasev D, Rahman IA, Garwood RJ, Spencer ART, Turner MJ, Kelleher JF (2018) Exploring the potential of neutron imaging for life sciences on IMAT. J Microsc 00(0):1–6
7. Caine RS, Yin X, Sloan J, Harrison EL, Mohammed U, Fulton T, Biswal AK, Dionora J, Chater CC, Coe RA, Bandyopadhyay A, Murchie EH, Swarup R, Quick WP, Gray JE (2019) Rice with reduced stomatal density conserves water and has improved drought tolerance under future climate conditions. New Phytol 221(1):371–384
8. Cao X, Xiao J, Wu M, Zeng W, Huang X (2021) Agricultural Water Use Efficiency and Driving Force Assessment to Improve Regional Productivity and Effectiveness. Water Resour Manage 35(8):2519–2535
9. Chapman N, Whalley WR, Lindsey K, Miller AJ (2011) Water supply and not nitrate concentration determines primary root growth in Arabidopsis. Plant Cell Environ 34(10):1630–1638
10. Dayod M, Aukett L, Henderson S, Tyerman SD, Shearer MK, Athman A, Fuentes S, Xu B, Conn SJ, Conn V, Gilliham M, Hocking B (2013) Protocol: optimising hydroponic growth systems for nutritional and physiological analysis of Arabidopsis thaliana and other plants. Plant Methods 9(1):4
11. Downie H, Holden N, Otten W, Spiers AJ, Valentine TA, Dupuy LX (2012) Transparent Soil for Imaging the Rhizosphere. PLoS ONE 7(9):1–6
12. Drakopoulos M, Connolley T, Reinhard C, Atwood R, Magdysyuk O, Vo N, Hart M, Connor L, Humphreys B, Howell G, Davies S, Hill T, Wilkin G, Pedersen U, Foster A, Maio N, De, Basham M, Yuan

F, Wanelik K (2017) beamlines I12: the Joint Engineering, Environment and Processing (JEEP) beamline at Diamond Light Source beamlines, (2015), 828–838

13. Dunn J, Hunt L, Afsharinafar M, Meselmani M, Al, Mitchell A, Howells R, Wallington E, Fleming AJ, Gray JE (2019) Reduced stomatal density in bread wheat leads to increased water-use efficiency.Journal of Experimental Botany
14. FAO (2020) The State of Food and Agriculture 2020. Overcoming water challenges in agriculture |Policy Support and Governance| Food and Agriculture Organization of the United Nations [online]. Available from: http://www.fao.org/policy-support/tools-and-publications/resources-details/en/c/1333955/ [Accessed 15 Jul 2021]
15. Farquhar GD, Ehleringer JR, Hubic KT, Farquhar GD, Ehleringer JR, Hubick KT (1989) Carbon isotope discrimination and photosynthesis. Plant Physiol 40:503–537
16. FEI (2015) User's guide Avizo ® 9 [online]
17. Franks PJ, Doheny-Adams W, Britton-Harper T, Gray JE (2015) Increasing water-use efficiency directly through genetic manipulation of stomatal density. New Phytol 207(1):188–195
18. French A, Ubeda-Tomas S, Holman TJ, Bennett MJ, Pridmore T (2009) High-Throughput Quantification of Root Growth Using a Novel Image-Analysis Tool. Plant Physiol 150(4):1784–1795
19. Gleick PH, Cooley H (2021) Freshwater Scarcity.Annual Review of Environment and Resources, 46 (1)
20. Helliwell JR, Sturrock CJ, Miller AJ, Whalley WR, Mooney SJ (2019) The role of plant species and soil condition in the structural development of the rhizosphere. Plant Cell Environ 42(6):1974–1986
21. Hepworth C, Doheny-adams T, Hunt L, Cameron DD, Gray JE (2015) Manipulating stomatal density enhances drought tolerance without deleterious effect on nutrient uptake. New Phytol 208:336–341
22. Hepworth C, Turner C, Landim MG, Cameron D, Gray JE (2016) Balancing Water Uptake and Loss through the Coordinated Regulation of Stomatal and Root Development.Plos One, 11 (6), e0156930
23. Hoogeveen J, Faurès J-M, Peiser L, Burke J, van de Giesen N (2015) GlobWat – a global water balance model to assess water use in irrigated agriculture. Hydrol Earth Syst Sci 19(9):3829–3844
24. Hughes J, Hepworth C, Dutton C, Dunn JA, Hunt L, Stephens J, Waugh R, Cameron DD, Gray JE (2017) Reducing stomatal density in barley improves drought tolerance without impacting on yield. Plant Physiol 174(2):776–787
25. Hunt L, Gray JE (2009) The Signaling Peptide EPF2 Controls Asymmetric Cell Divisions during Stomatal Development. Curr Biol 19(10):864–869
26. Iyer-Pascuzzi AS, Symonova O, Mileyko Y, Hao Y, Belcher H, Harer J, Weitz JS, Benfey PN (2010) Imaging and Analysis Platform for Automatic Phenotyping and Trait Ranking of Plant Root Systems. Plant Physiol 152(3):1148–1157
27. Lucas M, Swarup R, Paponov IA, Swarup K, Casimiro I, Lake D, Peret B, Zappala S, Mairhofer S, Whitworth M, Wang J, Ljung K, Marchant A, Sandberg G, Holdsworth MJ, Palme K, Pridmore T, Mooney S, Bennett MJ (2011) SHORT-ROOT Regulates Primary, Lateral, and Adventitious Root Development in Arabidopsis. Plant Physiol 155(January):384–398

28. Lundgren MR, Mathers A, Baillie AL, Dunn J, Wilson MJ, Hunt L, Pajor R, Fradera-Soler M, Rolfe S, Osborne CP, Sturrock CJ, Gray JE, Mooney SJ, Fleming AJ (2019) Mesophyll porosity is modulated by the presence of functional stomata. *Nature Communications 2019 10:1*, 10 (1), 1–10
29. Ma L, Shi Y, Siemianowski O, Yuan B, Egner TK, Mirnezami SV, Lind KR, Ganapathysubramanian B, Venditti V, Cademartiri L (2019) Hydrogel-based transparent soils for root phenotyping in vivo. Proc Natl Acad Sci USA 116(22):11063–11068
30. Mawodza T, Burca G, Casson S, Menon M (2020) Wheat root system architecture and soil moisture distribution in an aggregated soil using neutron computed tomography. Geoderma 359:113988
31. Mohammed U, Caine RS, Atkinson JA, Harrison EL, Wells D, Chater CC, Gray JE, Swarup R, Murchie EH (2019) Rice plants overexpressing OsEPF1 show reduced stomatal density and increased root cortical aerenchyma formation. Sci Rep 9(1):5584
32. Morris EC, Griffiths M, Golebiowska A, Mairhofer S, Burr-Hersey J, Goh T, Wangenheim D, Von, Atkinson B, Sturrock CJ, Lynch JP, Vissenberg K, Ritz K, Wells DM, Mooney SJ, Bennett MJ, von Wangenheim D, Atkinson B, Sturrock CJ, Lynch JP, Vissenberg K, Ritz K, Wells DM, Mooney SJ, Bennett MJ (2017) Shaping 3D Root System Architecture. Curr Biol 27(17):R919–R930
33. Ortas I (2008) Determination of the extent of rhizosphere soil. http://dx.doi.org/10.1080/*00103629709369914*, 28 (19–20), 1767–1776
34. Ramachandran GN, Lakshminarayanan AV (1971) Three-dimensional reconstruction from radiographs and electron micrographs: application of convolutions instead of Fourier transforms. Proc Natl Acad Sci USA 68(9):2236–2240
35. Schneider C, Rasband WS, Eliceiri KW (2012) NIH Image to ImageJ: 25 years of image analysis. Nat Methods 9(7):671–675
36. Seignez N, Gauthier A, Mess F, Brunel C, Dubois M, Potdevin JL (2010) Development of plant roots network in polluted soils: An x-ray computed microtomography investigation. Water Air Soil Pollut 209(1–4):199–207
37. Strehmel N, Böttcher C, Schmidt S, Scheel D (2014) Profiling of secondary metabolites in root exudates of Arabidopsis thaliana. Phytochemistry 108:35–46
38. Tracy SR, Roberts JA, Black CR, McNeill A, Davidson R, Mooney SJ (2010) The X-factor: Visualizing undisturbed root architecture in soils using X-ray computed tomography. J Exp Bot 61(2):311–313
39. UNESCO (2021) Valuing water - The United Nations World Water Development Report 2021.Water Politics,206
40. Wadeson N, Basham M (2016) In: Savu (ed) A Python-based, MPI Framework for Simultaneous Processing of Multiple, N-dimensional. Large Tomography Datasets
41. Xiao Q, De Gernier H, Kupcsik L, De Pessemier J, Dittert K, Fladung K, Verbruggen N, Hermans C (2015) Natural genetic variation of Arabidopsis thaliana root morphological response to magnesium supply. Crop and Pasture Science 66(12):1249–1258

Figures

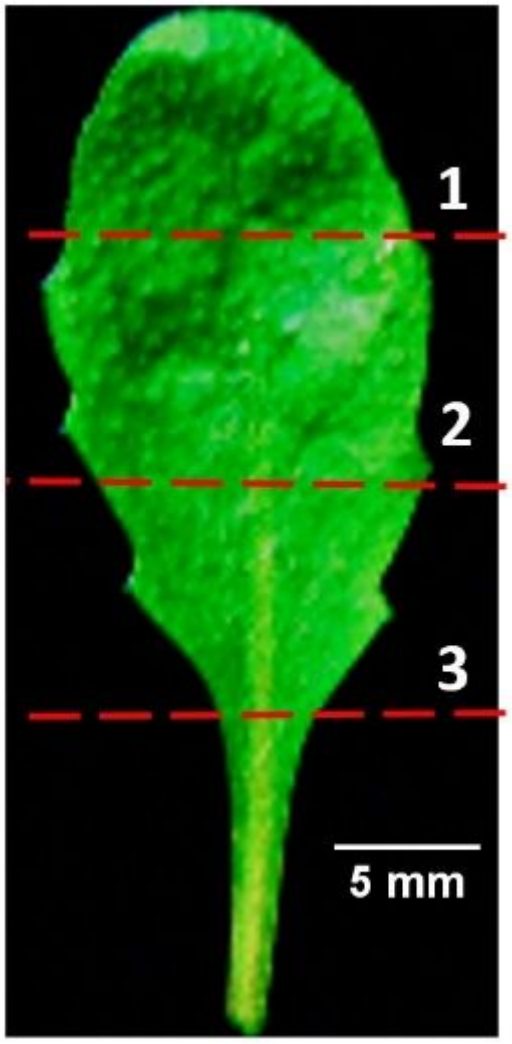

Figure 1

Sections of the Arabidopsis leaves where the different cell counts were made

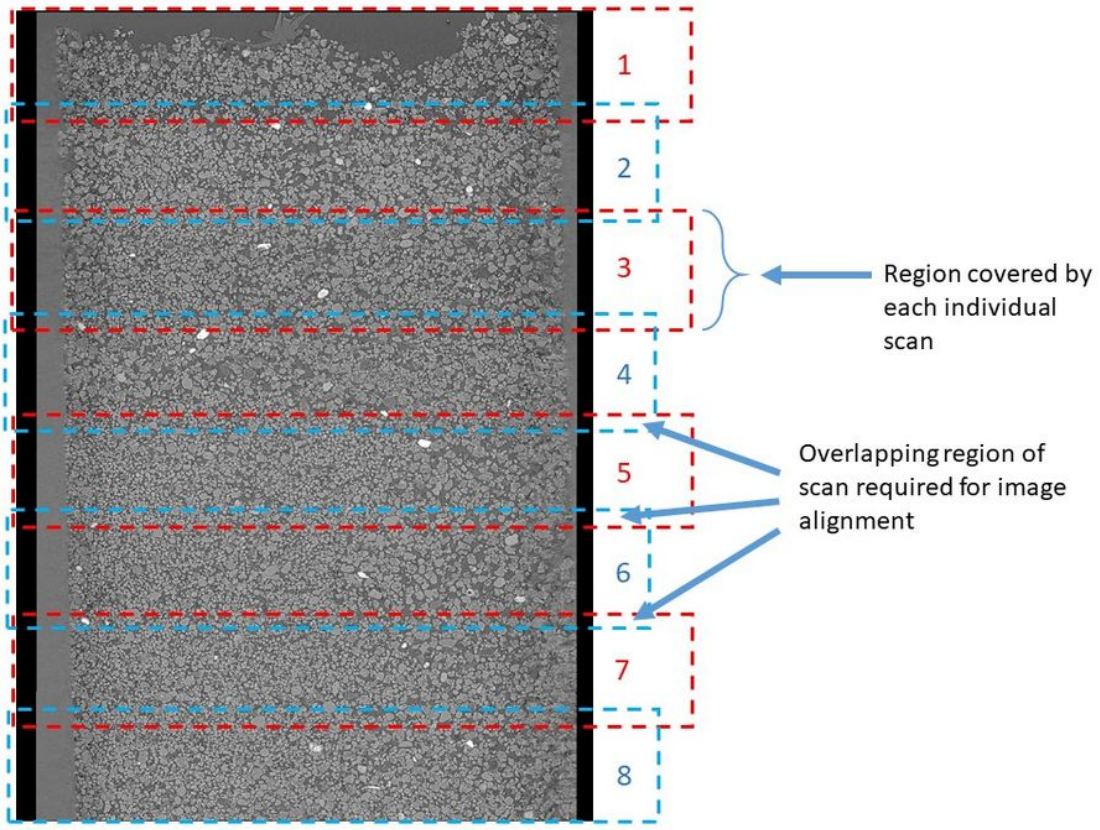

Figure 2

Image showing the 8 different regions covered by each scan which were subsequently reconstructed into a single stack.

Figure 3

Close up image 3D(left) and 2D(right) of an Arabidopsis root growing throught the soil with bulk (brown) and rhizosphere(highlight) soil clearly indicated (scale bar = 200µm).

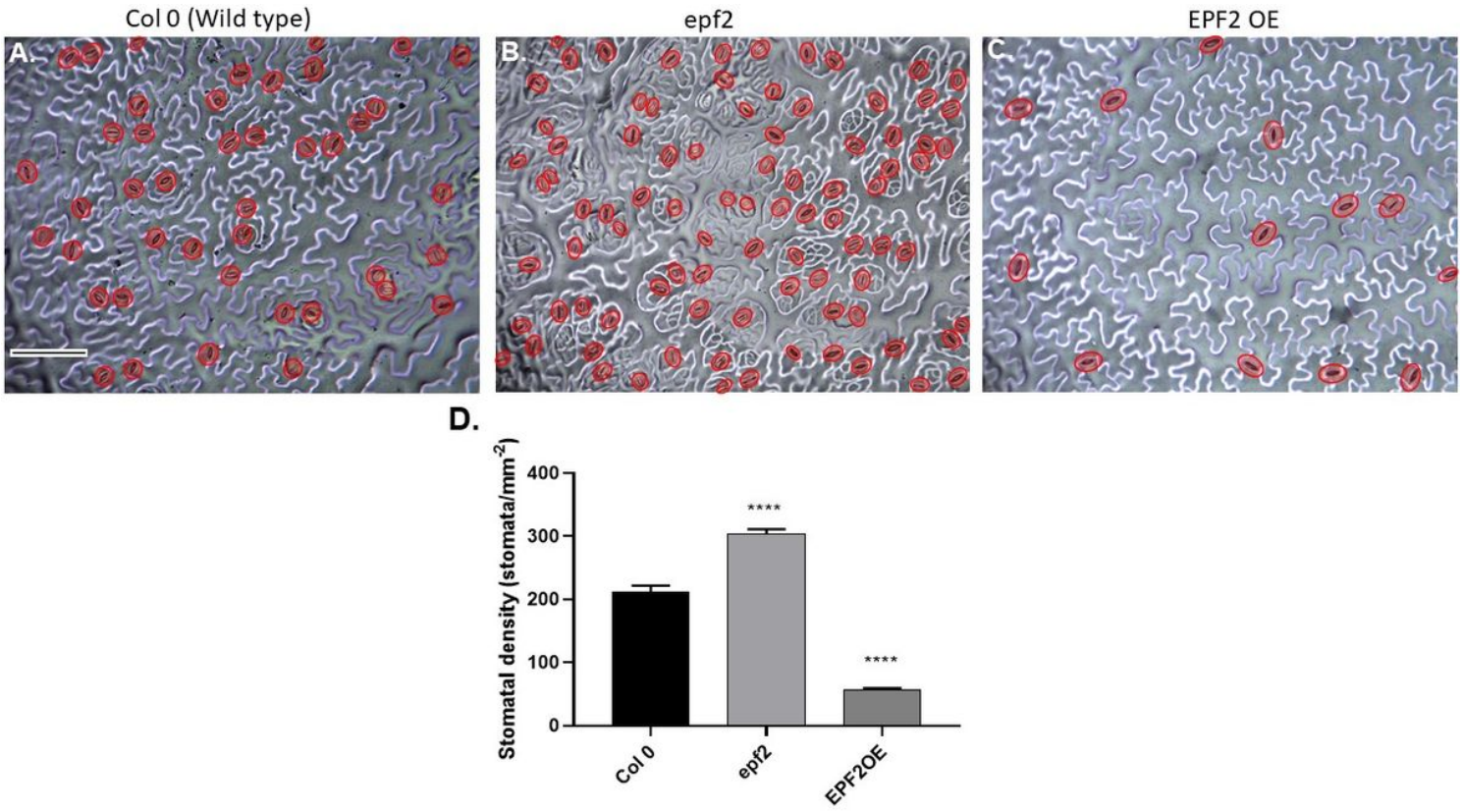

Figure 4

(A-C) Stomatal density of the abaxial Arabidopsis surface (bar indicates 100 µm). D Stomatal density Arabidopsis surface of different mutants. Error bars indicate standard error of the Mean (SEM). Symbols indicate significant difference as compared to Col-0; (*=≤0.05, ****= ≤0.0001)

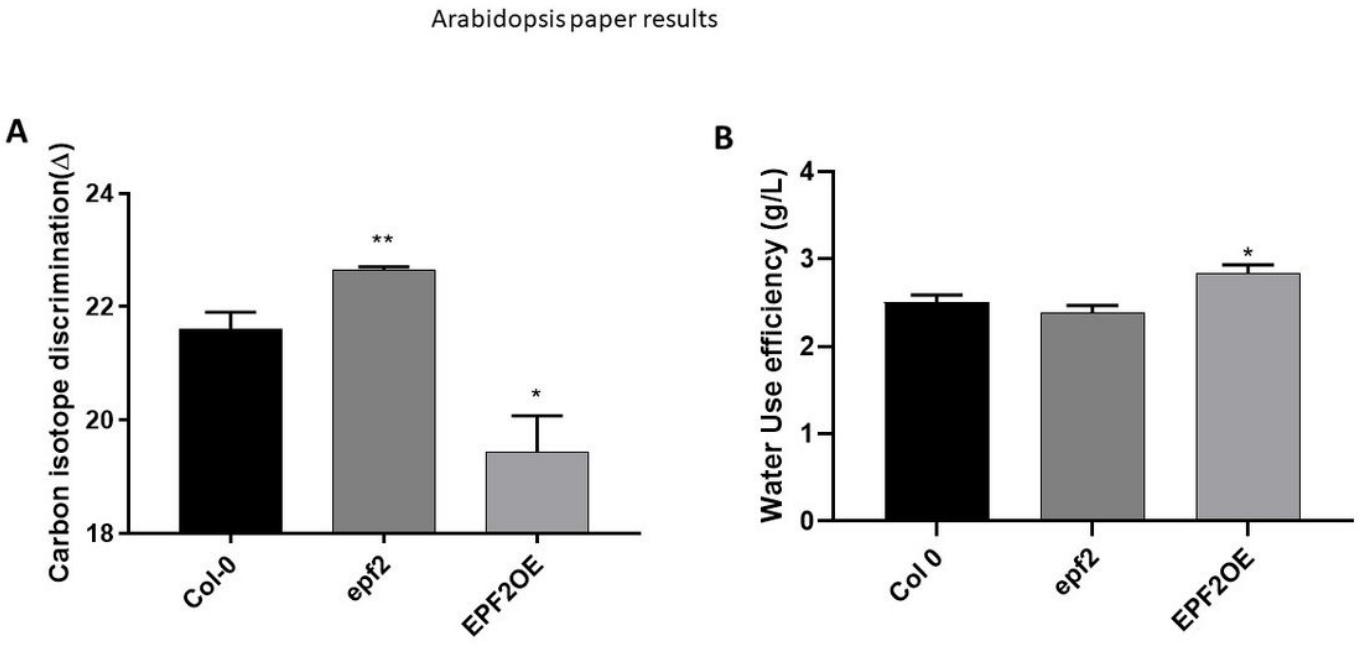

Figure 5

Water use efficiency as estimated by A) Carbon isotope discrimination and B) Biomass to water transpiration in Arabidopsis plants grown until maturity (n≥3). Error bars indicate standard error of the Mean (SEM). Symbols indicate significant difference as compared to Col-0; (*=≤0.05. **= ≤0.01)

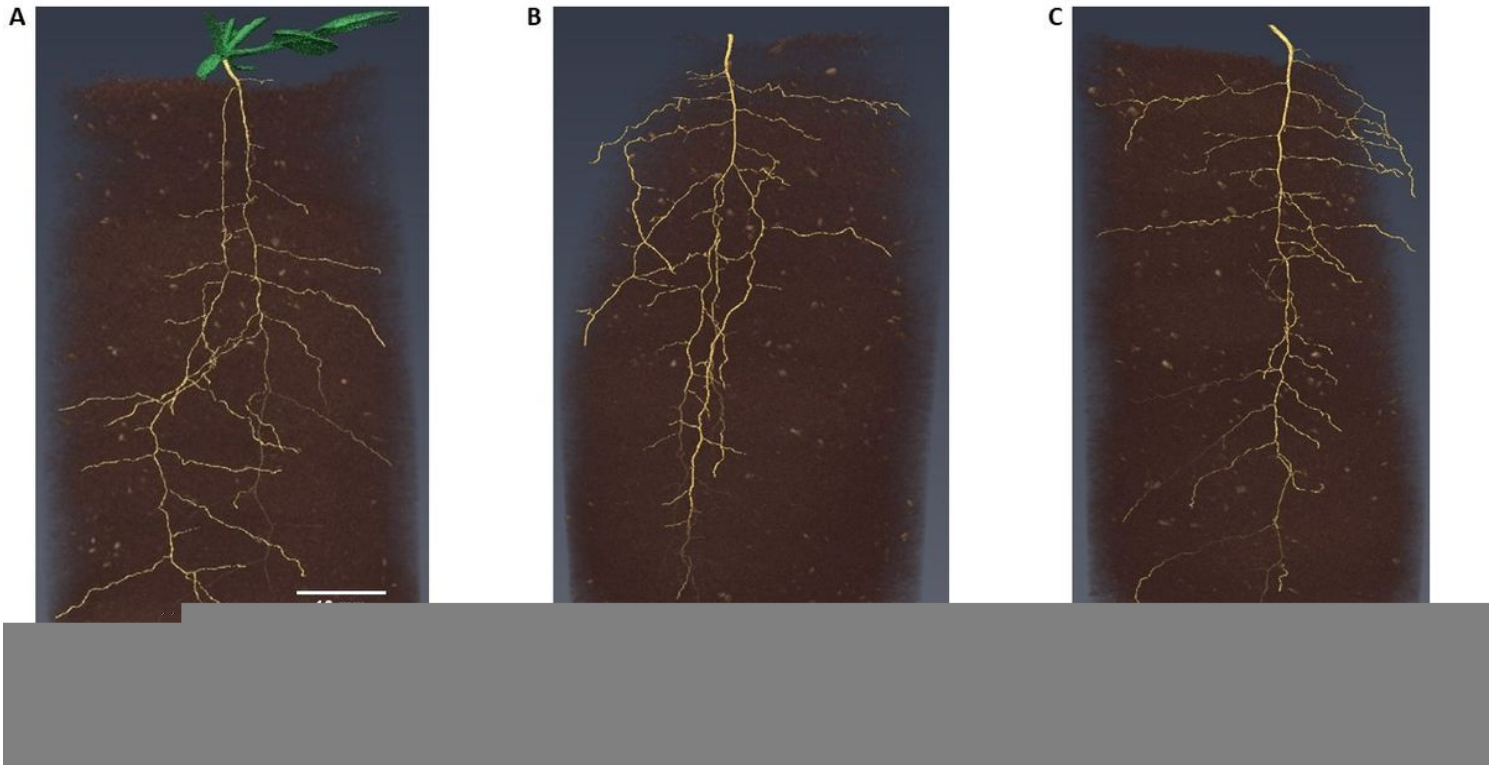

Figure 6

Three dimensional rendering of the different Arabidopsis genotypes from sX-Ray CT scanning

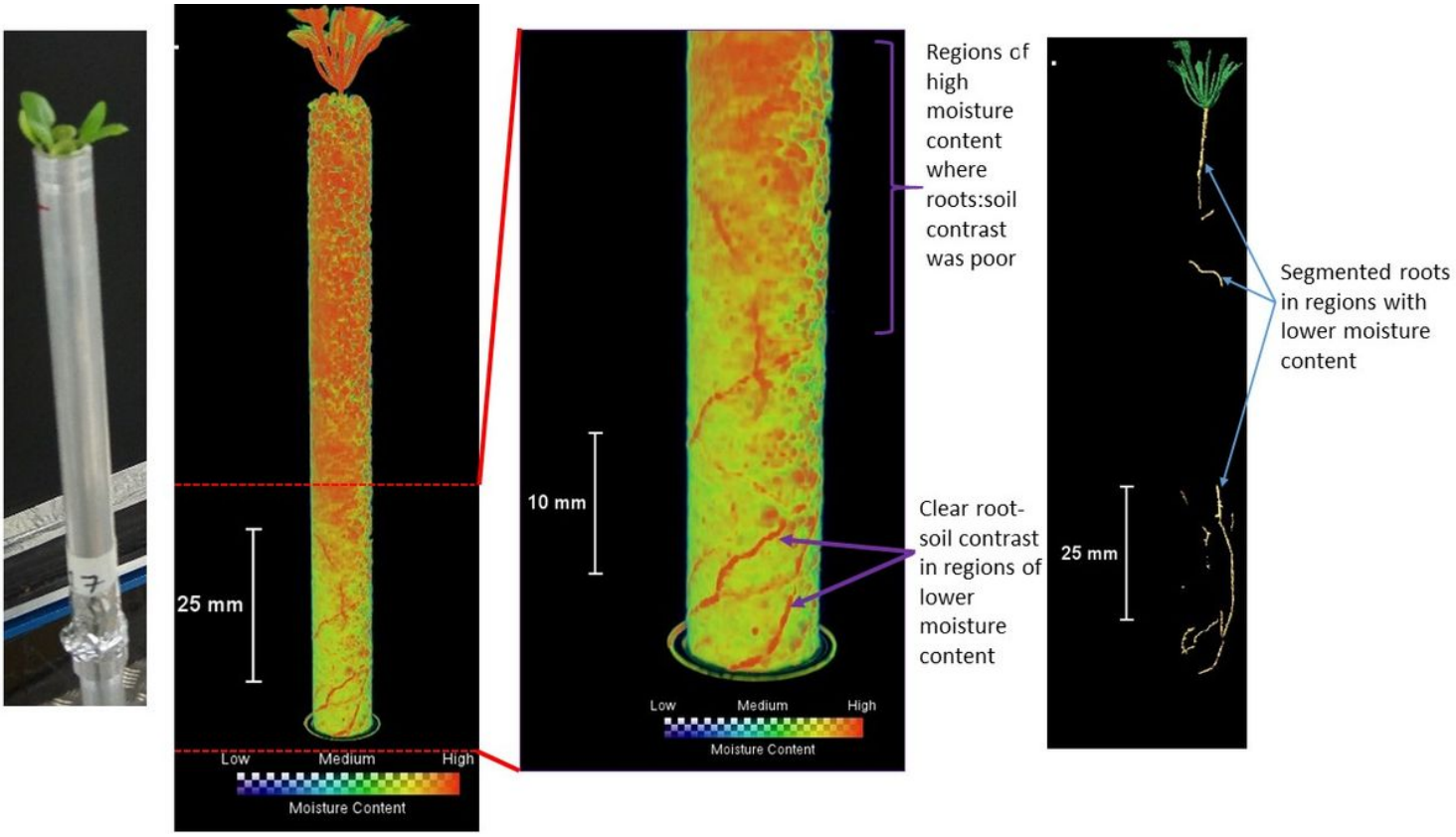

Figure 7

Arabidopsis root NCT image showing regions of high soil moisture (orange zones) which prevented accurate root segmentation. Roots distinct and large enough to segment are shown on the extreme right.

Figure 8

Root properties of Arabidopsis plants grown in a sandy loam soil as derived from XRSI, (A) Root length, (B) volume, (C) diameter (D) Lateral roots per primary root (E) convex hull volume, (F) lateral root angle (n=3)

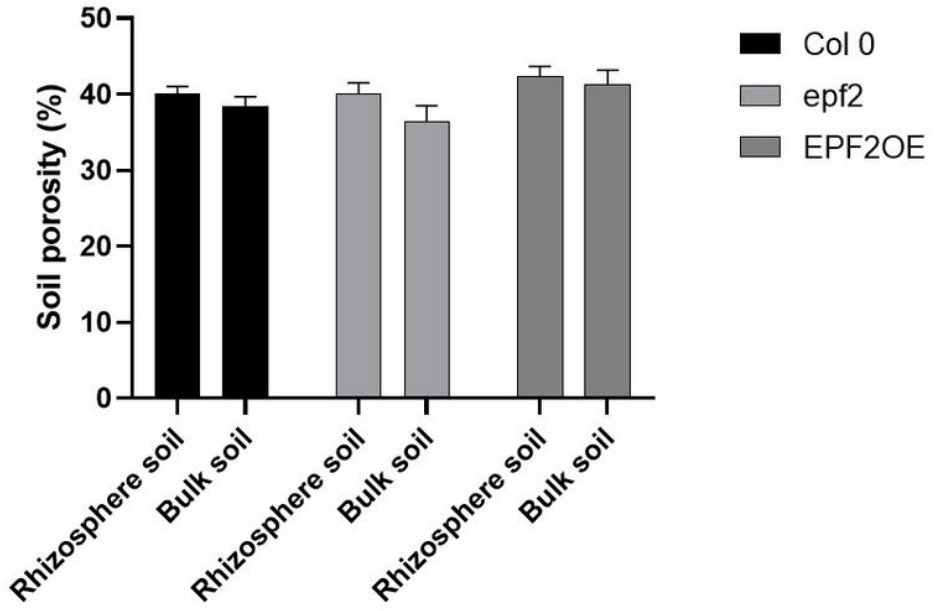

Figure 9

Soil porosity differences between rhizosphere and bulk soil for each of the genotypes (n=3)